Near-edge structures from first principles all-electron Bethe–Salpeter equation calculations

2009 J. Phys.: Condens. Matter 21 104205

(http://iopscience.iop.org/0953-8984/21/10/104205)

IOP Publishing Journal of Physics: Condensed Matter

J. Phys.: Condens. Matter **21** (2009) 104205 (6pp) doi:10.1088/0953-8984/21/10/104205

Near-edge structures from first principles all-electron Bethe–Salpeter equation calculations

W Olovsson[1], I Tanaka[1,2], P Puschnig[3] and C Ambrosch-Draxl[3]

[1] Department of Materials Science and Engineering, Kyoto University, Sakyo, Kyoto 606-8501, Japan
[2] Nanostructures Research Laboratory, Japan Fine Ceramics Centre, Atsuta, Nagoya 456-8587, Japan
[3] Chair of Atomistic Modelling and Design of Materials, Montanuniversität Leoben, Franz-Josef-Straße 18, A-8700 Leoben, Austria

E-mail: weine@phd.mbox.media.kyoto-u.ac.jp

Received 23 October 2008, in final form 27 November 2008
Published 10 February 2009
Online at stacks.iop.org/JPhysCM/21/104205

Abstract

We obtain x-ray absorption near-edge structures (XANES) by solving the equation of motion for the two-particle Green's function for the electron–hole pair, the Bethe–Salpeter equation (BSE), within the all-electron full-potential linearized augmented plane wave method (FPLAPW). The excited states are calculated for the Li K-edge in the insulating solids LiF, Li_2O and Li_2S, and absorption spectra are compared with independent particle results using the random phase approximation (RPA), as well as supercell calculations using the core-hole approximation within density functional theory (DFT). The binding energies of strongly bound excitations are determined in the materials, and core-exciton wavefunctions are demonstrated for LiF.

(Some figures in this article are in colour only in the electronic version)

1. Introduction

The near-edge structure spectroscopies, x-ray absorption spectroscopy (XANES) and electron energy loss spectroscopy (ELNES)—an increasingly popular spectroscopy in the connection with transmission electron microscopy (TEM)—give valuable information about the chemical properties and electronic structure of materials by probing their excited states [1, 2]. In semiconductors and insulators, the band-gap allows for the creation of bound core-excitons due to the imperfect screening of the Coulomb interaction between the core hole and excited electron simultaneously created in the absorption process. For the near-edge structure region, within roughly 40 eV from the edge, excitonic effects have a large impact on the absorption rate for bound core-excitons as well as higher energy excitations. With the improvement of experimental design and higher instrumental resolution in spectroscopy, it is of interest to evaluate theoretical methods for reproducing the absorption spectra, to compare different approaches, and to investigate the level of accuracy needed to describe the near-edge structure.

In order to include excitonic effects in theoretical spectra, we consider the equation of motion for the electron–hole (e–h) pair using the two-particle Green's function, the Bethe–Salpeter equation (BSE) [3–8], based on the all-electron full-potential linearized augmented plane wave method (FPLAPW) [9] utilizing the `WIEN2k` program package [10]. The present scheme has been successfully applied to the optic region [11], and very recently to XANES [12]. Here, the frozen core approximation is not employed in the calculations and the excited states are explicitly determined, i.e. energies and oscillator strengths are obtained together with the corresponding wavefunctions for the excitations. While a BSE scheme based on the pseudopotential method was previously used for obtaining the absorption spectra [13–15] it is, however, still much more common in the literature to rely on single-particle theory. A popular method is to perform density functional theory (DFT) [16, 17] calculations and explicitly introduce a core hole at a single atom in a supercell of atoms, see, for example, [1, 2]. Such supercell techniques using the core-hole approximation provide comparatively fast ways to estimate the x-ray absorption spectra, often with a reasonable

agreement with experiment, especially considering the deep core region [18]. Still, BSE constitutes a rigorous approach based on many body perturbation theory, which goes beyond single-particle approximations for the inclusion of excitonic effects.

To demonstrate our method, the XANES spectra are presently obtained in insulating lithium compounds, considering the Li K-edge for LiF, Li_2O and Li_2S, by computing the excited states within the formalism of the all-electron FPLAPW Bethe–Salpeter equation. The effect of e–h interaction and exchange on the spectra is shown by comparison between BSE and independent particle results in the random phase approximation (RPA). Results using DFT supercell techniques with the core-hole approximation are also shown. In addition, the binding energy of bound core-exciton states is calculated and examples of the corresponding exciton wavefunctions in LiF are given. The near-edge structure of LiF and other Li-halides has attracted interest over the decades (see for instance the earlier results and discussion in [19–29] and more recent work [12, 14, 15, 30–33]). Li_2O has recently been studied in [32, 34–37] and is of interest for practical applications, including optical glass and solid state batteries. One may note that LiF and Li_2O exemplify simple ionic and oxide materials whose investigation might be valuable as a basis for understanding more complex compounds.

2. Methodology

The Bethe–Salpeter equation [3–8] has previously been calculated in a first principles manner for the optic [11, 40–44] and x-ray [12–15] regimes of the absorption spectra. A full review on BSE together with the alternative method of time-dependent DFT can be found in [38]. Our scheme is described in more detail in [11, 39] considering the optic region, which is analogous to the present treatment.

Starting eigenenergies and wavefunctions for the electron and hole states needed in the BSE scheme are generated within DFT [16, 17], by self-consistently solving the Kohn–Sham equations using the all-electron FPLAPW [9] code `WIEN2k` [10]. In APW methods the basis set is split into atomic-like wavefunctions inside non-overlapping spheres centered on the atoms and plane waves in the leftover interstitial region. For the present calculations a cutoff $RK_{\max} = 7$ was used for the basis set, where R denotes the radius of the atomic sphere and $K_{\max}$ is the magnitude of the largest $\mathbf{k}$-vector for the plane waves [10]. Supercell calculations utilizing the core-hole approximation were also performed using the `WIEN2k` code, with 64 atoms for LiF and 96 atoms for Li_2O and Li_2S, respectively. Further information concerning the LAPW methods can be found in [45, 46]. The crystal structures are rock salt for LiF and anti-fluorite for Li_2O and Li_2S. The generalized gradient approximation (GGA) [47] was selected to describe the exchange–correlation effects in DFT, and experimental lattice parameters were used in the calculations.

In order to compute the excited states and obtain the absorption spectra, the BSE is first reformulated into an effective Hamiltonian acting on a selected range of hole and electron states. It can be shown that the matrix elements for the e–h pairs adopt a block-form

$$H = \begin{pmatrix} R & C \\ -C^* & -R^* \end{pmatrix}, \tag{1}$$

where R corresponds to the resonant (ω) and $-R^*$ to the anti-resonant ($-\omega$) parts, with the coupling C and $-C^*$ between them. Here we use the Tamm–Dancoff approximation [48], i.e. setting the coupling $C = 0$, which except for the sign gives the same solutions for the two blocks. Now considering only the resonant positive frequencies, and assuming no spin–orbit coupling, the solution of an effective two-particle Hamiltonian H^{eh} splits into spin-singlet and triplet, with the singlet

$$H^{\mathrm{eh}} = H^{\mathrm{diag}} + H^{\mathrm{dir}} + 2H^{x}. \tag{2}$$

Starting with the diagonal term,

$$H^{\mathrm{diag}} = (E_{\beta\mathbf{k}} - E_{\alpha\mathbf{k}})\delta_{\alpha\alpha'}\delta_{\beta\beta'}\delta_{\mathbf{k}\mathbf{k}'}, \tag{3}$$

it only contains the difference in the quasi-particle eigenenergies between the hole (α), $E_{\alpha\mathbf{k}}$, and electron (β) states, $E_{\beta\mathbf{k}}$, where $\mathbf{k}$ is a wavevector inside the Brillouin zone. Solved separately it produces the result for independent particles with no interaction, corresponding to the random phase approximation without crystal local field corrections. H^{dir} stands for the direct term

$$H^{\mathrm{dir}}_{\alpha\beta\mathbf{k},\alpha'\beta'\mathbf{k}'} = -\int \mathrm{d}^3r\,\mathrm{d}^3r'\,\psi_{\alpha\mathbf{k}}(\mathbf{r})\psi^*_{\beta\mathbf{k}}(\mathbf{r}')W(\mathbf{r},\mathbf{r}')\psi^*_{\alpha'\mathbf{k}'}(\mathbf{r})\psi_{\beta'\mathbf{k}'}(\mathbf{r}'), \tag{4}$$

which introduces the attractive screened static Coulomb interaction W, responsible for the creation of bound core-exciton states. W is related to the inverse microscopic dielectric matrix, $W \propto \varepsilon^{-1}$, which is calculated from the static, irreducible polarization within the RPA. One may note that in metallic systems it would be important to consider dynamic (frequency-dependent) effects [49]. The last term, H^{x}, is the exchange for the e–h pairs

$$H^{x}_{\alpha\beta\mathbf{k},\alpha'\beta'\mathbf{k}'} = \int \mathrm{d}^3r\,\mathrm{d}^3r'\,\psi_{\alpha\mathbf{k}}(\mathbf{r})\psi^*_{\beta\mathbf{k}}(\mathbf{r})\bar{v}(\mathbf{r},\mathbf{r}')\psi^*_{\alpha'\mathbf{k}'}(\mathbf{r}')\psi_{\beta'\mathbf{k}'}(\mathbf{r}'), \tag{5}$$

with the bare Coulomb potential, $\bar{v}$, where only the short-range part needs to be taken into account. In the case of no spin–orbit coupling the exchange is only present for the spin-singlet. The solution for triplets (which is a forbidden transition, since spin is not conserved) reduces to $H^{\mathrm{eh}} = H^{\mathrm{diag}} + H^{\mathrm{dir}}$. By itself the exchange term produces the full RPA, including crystal local field corrections.

After calculating the matrix elements for a selected range of hole and electron states in (3)–(5), the BSE can be solved by considering the matrix eigenvalue equation

$$\sum_{\alpha'\beta'\mathbf{k}'} H^{\mathrm{eh}}_{\alpha\beta\mathbf{k},\alpha'\beta'\mathbf{k}'}A^{\lambda}_{\alpha'\beta'\mathbf{k}'} = E^{\lambda}A^{\lambda}_{\alpha\beta\mathbf{k}}, \tag{6}$$

where E^{λ} is the eigenenergy. $A^{\lambda}_{\alpha\beta\mathbf{k}}$ are the eigenvectors, acting as coupling coefficients for the e–h pairs contributing

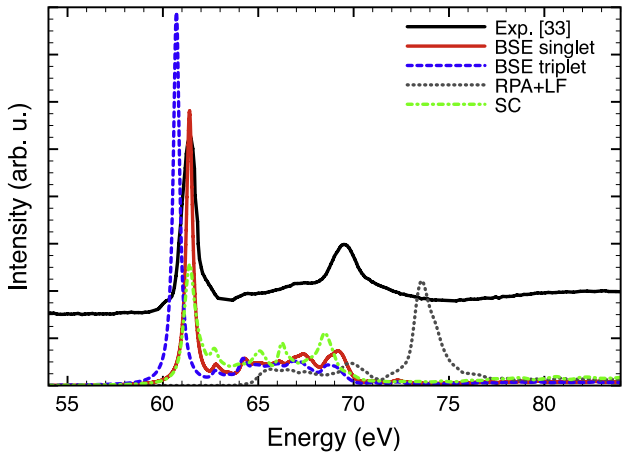

Figure 1. The XANES spectra for the Li K-edge in LiF. The BSE spin-singlet (red (gray) line) is compared to the triplet (dashed blue line), full RPA with crystal local field corrections (dotted gray line) and supercell calculations with core-hole approximation (dot-dashed green line), together with experiment (thick black line).

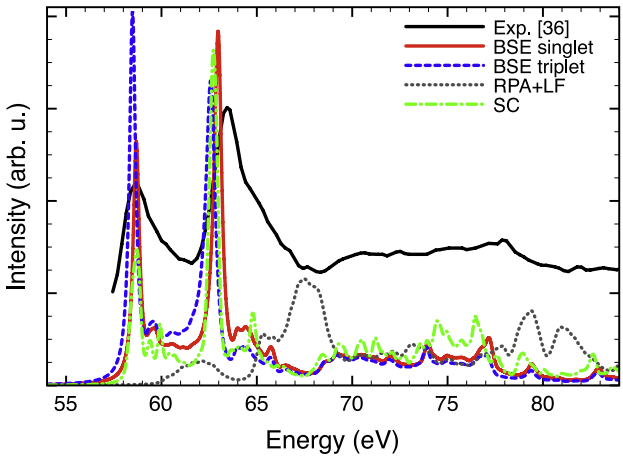

Figure 2. The absorption spectra for the Li K-edge in Li_2O. The same notation as in figure 1 is used.

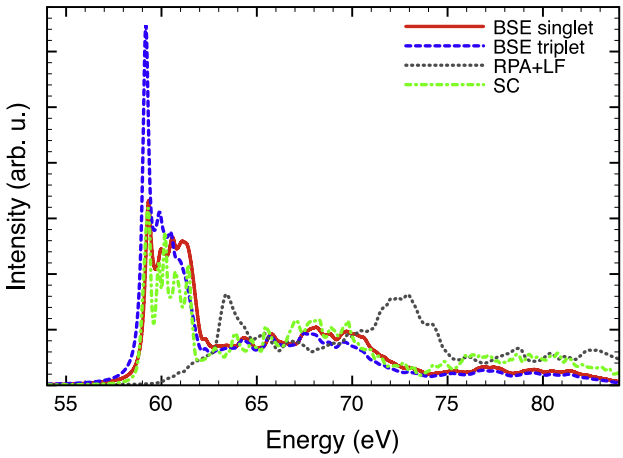

Figure 3. The absorption spectra for the Li K-edge in Li_2S. Same notation as in figure 1.

to the excitation λ. The excitations are numbered according to the absorption spectra, going from lower (more bound) to higher energies (less bound and unbound). The correlated electron–hole wavefunction can be constructed from a coherent sum over single-particle e–h states weighted by the coupling coefficients A

$$\Phi^{\lambda}(\mathbf{r}_e, \mathbf{r}_h) = \sum_{\alpha\beta\mathbf{k}} A^{\lambda}_{\alpha\beta\mathbf{k}} \psi^{*}_{\alpha\mathbf{k}}(\mathbf{r}_h)\psi_{\beta\mathbf{k}}(\mathbf{r}_e), \qquad (7)$$

$\mathbf{r}_e$ and $\mathbf{r}_h$ denote the real-space coordinates of the electron and hole, and ψ refers to the respective single-particle wavefunctions. As the effective two-particle Hamiltonian in (6) is solved, the absorption spectra can now be obtained from the imaginary part of the dielectric tensor

$$\varepsilon_2(\omega) \propto \sum_{\lambda} \left| \sum_{\alpha\beta\mathbf{k}} A^{\lambda}_{\alpha\beta\mathbf{k}} \frac{\langle \alpha\mathbf{k}|p|\beta\mathbf{k}\rangle}{\varepsilon_{\alpha\mathbf{k}} - \varepsilon_{\beta\mathbf{k}}} \right|^2 \times \delta(E^{\lambda} - \omega), \qquad (8)$$

where p is the momentum operator in the electric dipole approximation ($\Delta l \pm 1$), and $\langle \alpha\mathbf{k}|p|\beta\mathbf{k}\rangle$ are the transition matrix elements. We approximate the quasi-particle energies by Kohn–Sham energies.

For a sufficient convergence of the features in the absorption spectra and to determine the core-exciton binding energies, a shifted $10 \times 10 \times 10$ **k**-mesh with 47 irreducible **k**-points was selected to calculate the static screened Coulomb interaction W, as well as the matrix elements in H^{eh}, for Li_2O and Li_2S. A slightly denser mesh, $11 \times 11 \times 11$ with 56 irreducible **k**-points, was applied in the case of LiF. The cutoffs $\mathbf{G}_{\max} = 4.0\,\mathrm{bohr}^{-1}$ for the reciprocal lattice parameter together with $l_{\max} = 2$ were used [11, 39], and the dielectric matrix was obtained including conduction states up to $E_{\max} = 20$ Ryd. The computations were made over the respective Li 1s (one for LiF and two for Li_2O and Li_2S) corresponding to the hole states and a selected range of unoccupied states, 15 (LiF), 17 (Li_2O) and 20 (Li_2S) for the electrons. In the last step, a Lorentzian broadening of $\sigma = 0.2$ eV was applied and the theoretical spectra aligned with experiment. Note that while the present methodology considers the near-edge structures in x-ray absorption, ELNES produces similar spectra in the limit of small momentum transfer ($q \to 0$) (see for example [2]).

3. Results and discussion

The excited states together with the corresponding XANES spectra are calculated using the all-electron FPLAPW BSE code for the Li K-edge, starting with LiF in figure 1 and Li_2O and Li_2S in figure 2, respectively 3. Because spin–orbit coupling is not considered in the present work, there is a straightforward separation of the BSE results into spin-singlet (red (gray) line) and the spin-forbidden triplet states (dashed blue line), which does not include the exchange term. The result for independent particles can be expressed in the random phase approximation by solving equation (6) for the diagonal term. By only keeping the exchange, the full RPA with crystal local field corrections (dotted gray line) is obtained, here shown in the figures for comparison to BSE. DFT supercell calculations with the core-hole approximation

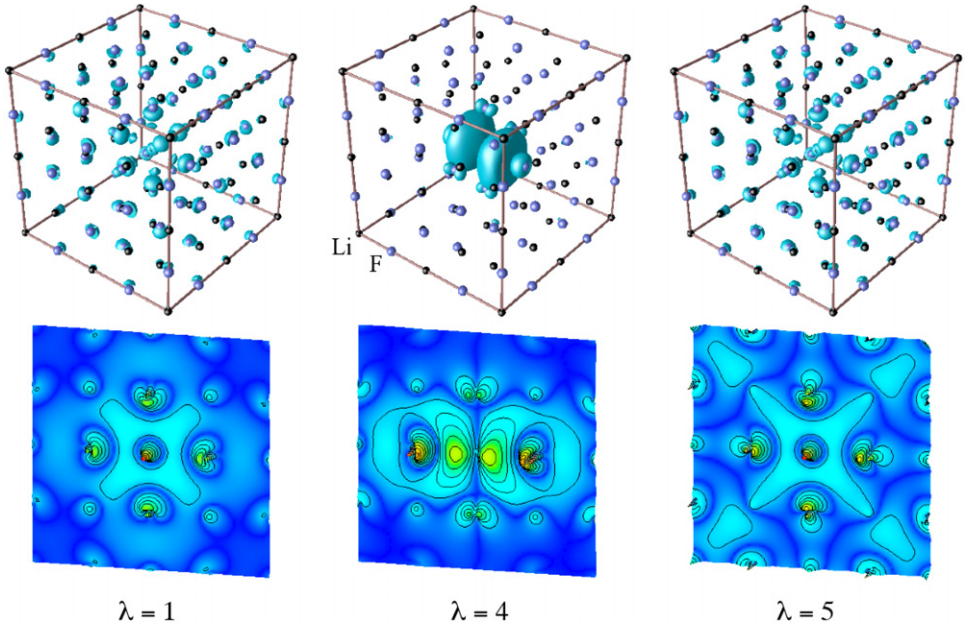

Figure 4. The real-space wavefunctions are shown for the Li K-edge bound core-excitons in rock salt LiF, with the hole located at the central Li atom. In the upper part, an isosurface is plotted for the absolute value of the wavefunction. Directly below, a contour plot is made for the (001)-plane through the central Li atom. $\lambda = 1$ and 5 correspond to the s-like core-excitons ($E_b = 2.4$ and 0.8 eV) and $\lambda = 4$ is one of the three degenerate p-like excitons ($E_b = 2.1$ eV).

Table 1. Theoretical binding energies for the strongest bound s- and p-orbital like core-excitons of the Li K-edge (eV).

	LiF	Li_2O	Li_2S
s	2.4	1.3	0.7
p	2.1	1.2	0.7

are also shown (dot-dashed green line). Theoretical results are displayed together with experiment (black thick line) for LiF and Li_2O [33, 36]. The binding energies for the strongest bound core-excitons of s- (with effectively zero transition probability in XANES), respectively p-orbital character are presented in table 1.

The interpretation of the near-edge structure features in LiF and the other Li-halides was much discussed around the 1970s [19–27]. Since then, several theoretical estimations of the absorption spectra have been made, for instance using the $(Z + 1)$-approximation for the core-hole [28] and molecular-orbital calculations [31]. Only recently, many-body perturbation theory in the form of pseudopotential BSE was applied for LiF [15, 30], and the remaining Li-halides [14]. In our previous work [12], the core-excitonic effects for the shallow core edges were studied, contrasting all-electron BSE results with supercell calculations using the core-hole approximation. It was noticed that the two different BSE approaches give a similar result, at least in the case of Li-halides. Turning to the computed spectra in figure 1, BSE produces a sharp excitonic edge followed by a detailed fine structure. Though the peak around ∼69 eV appears stronger in experiment, the general agreement with theory is good. In wide band-gap insulators such as LiF strong excitonic effects are to be expected. This is immediately realized by comparing BSE with the RPA, which does not include any expression for the Coulomb interaction between core hole and excited electron, and therefore does not give rise to bound states. The overall effect of the exchange term is to reduce the attractive screened Coulomb interaction, which is clearly seen from the difference in BSE singlet and triplet solutions for LiF. It reduces the oscillator strength and binding energy for the core-excitonic edge peak in the allowed singlet transition. While the supercell results approximate the general shape of the experimental spectra, the peaks appear shifted in comparison with BSE [12]. On a closer look, a pre-edge structure at the main peak is found in experiment. It is usually attributed to lattice vibrations, which break the crystal symmetry slightly, allowing transition to the strongly bound s-like exciton ($\lambda = 1$).

The XANES spectra for the Li K-edge in Li_2O and Li_2S are shown in figures 2 and 3. Previous theoretical investigations on the near-edge structures include the use of a molecular-orbital method [32], and supercell calculations with the core-hole approximation in the case of Li_2O [35, 36]. Also, the electron energy loss (EELS) spectra over a wide energy region were investigated regarding the crystal local field effects within the RPA for Li_2O (as well as LiF) [37]. Considering many-body theory results, the excitonic effects in Li_2O were first highlighted in [12], while Li_2S has so far not been studied. Going to the absorption spectra, as expected, the complete difference between BSE and RPA demonstrates the strong influence of the attractive interaction between the core hole and excited electrons. The effect of exchange is smaller for Li_2O and Li_2S than in LiF, though there is still a clear redistribution of oscillator strengths in the near-edge structure. One can note that in contrast to LiF, supercell techniques using the core-hole approximation give a reasonable estimation of

the experimental spectra in Li_2O (see for instance the direct comparison between many body theory and single-particle results in [12]). A rough similarity between BSE and supercell calculations with the core-hole approximation is also found for Li_2S. While Li_2O displays two marked peaks in the absorption spectra, where the strongest peak is not the edge peak, a more compact fine structure close to the edge is obtained for Li_2S. It was previously noted in [35] that a so-called pseudo-gap exists for the DFT p unoccupied states not far from the conduction band minimum for Li_2O, which here is realized as a gap in the RPA spectra (figure 2). By using the all-electron BSE, it was found that the transitions contributing to the dominating peak in Li_2O have the characteristics of both bound core-exciton states with higher oscillation strength and unbound excitations close in energy. Inspecting the RPA results for Li_2S in figure 3, this effect seems to be of less importance, and the absorption spectra have a different shape in comparison.

An advantage of the present BSE method is that the core-exciton wavefunction $\Phi^{\lambda}(\mathbf{r}_e, \mathbf{r}_h)$ can be determined from the various contributing e–h pairs by using equation (7). This gives the opportunity of analyzing the excitations in more detail by considering their extent and specific distribution in real-space. In figure 4, a demonstration is made for bound core-excitons in LiF, plotting the absolute value of the real-space wavefunction of the excited electron in relation to the fixed core hole at the Li atom in the center of the cell. Here a denser **k**-mesh was used compared with the previous calculations of the absorption spectra. A cutoff $|A^{\lambda}_{\alpha\beta\mathbf{k}}| = 0.01$ was imposed for the coupling coefficients, limiting the number of terms to $\sim 10^4$. $\lambda = 1$ and 5 in figure 4 correspond to s-like excitons with effectively zero oscillation strength, while the degenerate p-like states $\lambda = 2$–4 ($\lambda = 4$ shown in figure 4) are responsible for the sharp edged peak in figure 1. In comparison, the bound core-excitons in Li_2O, respectively Li_2S, were found to have a more complex structure, of a larger extent in real-space and with Li_2S the largest, but still of a localized character.

4. Conclusion

We demonstrated an all-electron Bethe–Salpeter equation scheme within the formalism of FPLAPW for the computation of excited states and XANES spectra, considering the Li K-edge in the insulating solids LiF, Li_2O and Li_2S. Spectra were obtained for spin-singlet and triplet states, showing the effect of exchange, and with comparison to the full RPA with crystal local field corrections and supercell calculations using the core-hole approximation within density functional theory. In addition, core-exciton binding energies were calculated in the materials, as well as exciton wavefunctions exemplified for LiF.

Acknowledgments

WO acknowledges financial support from the Japan Society for the Promotion of Science (JSPS). The presented work was supported by Grant-in-Aid for Scientific Research on Priority Areas 'Nano Materials Science for Atomic Scale Modification 474' from the Ministry of Education, Culture, Sports, Science and Technology (MEXT) of Japan and the Austrian Science Fund, project P16227.

References

[1] Tanaka I and Mizoguchi T 2009 *J. Phys.: Condens. Matter* **21** 104201
[2] Tanaka I, Mizoguchi T and Yamamoto T 2005 *J. Am. Ceram. Soc.* **88** 2013
[3] Sham L J and Rice T M 1966 *Phys. Rev.* **144** 708
[4] Hanke W and Sham L J 1975 *Phys. Rev.* B **12** 4501
[5] Hanke W and Sham L J 1979 *Phys. Rev. Lett.* **43** 387
[6] Hanke W and Sham L J 1980 *Phys. Rev.* B **21** 4656
[7] Strinati G 1982 *Phys. Rev. Lett.* **49** 1519
[8] Strinati G 1984 *Phys. Rev.* B **29** 5718
[9] Andersen O K 1975 *Phys. Rev.* B **12** 3060
[10] Blaha P, Schwartz K, Madsen G, Kvasnicka D and Luitz J 2001 *WIEN2k An Augmented Plane Wave Plus Local Orbitals Program for Calculating Crystal Properties* ed K Schwartz (Vienna: Technische Universität Wien)
[11] Puschnig P and Ambrosch-Draxl C 2002 *Phys. Rev.* B **66** 165105
[12] Olovsson W, Tanaka I, Mizoguchi T, Puschnig P and Ambrosch-Draxl C 2009 *Phys. Rev.* B **79** 041102
[13] Shirley E L 1998 *Phys. Rev. Lett.* **80** 794
[14] Shirley E L 2004 *J. Electron Spectrosc. Relat. Phenom.* **137** 579
[15] Soininen J A and Shirley E L 2001 *Phys. Rev.* B **64** 165112
[16] Hohenberg P and Kohn W 1964 *Phys. Rev.* B **136** 864
[17] Kohn W and Sham L J 1965 *Phys. Rev.* A **140** 1133
[18] Rehr J J, Soininen J A and Shirley E L 2005 *Phys. Scr.* T **115** 207
[19] Haensel R, Kunz C and Sonntag B 1968 *Phys. Rev. Lett.* **20** 262
[20] Brown F C, Gähwiller C, Kunz A B and Lipari N O 1970 *Phys. Rev. Lett.* **25** 927
[21] Kunz A B, Mickish D J and Collins T C 1973 *Phys. Rev. Lett.* **31** 756
[22] Sonntag B F 1974 *Phys. Rev.* B **9** 3601
[23] Gudat W, Kunz C and Petersen H 1974 *Phys. Rev. Lett.* **32** 1370
[24] Pantelides S T and Brown F C 1974 *Phys. Rev. Lett.* **33** 298
[25] Pantelides S T 1975 *Phys. Rev.* B **11** 239
[26] Fields J R, Gibbons P C and Schnatterly S E 1977 *Phys. Rev. Lett.* **38** 430
[27] Stott J P, Hilbert S L, Brown F C, Bunker B, Chiang T C, Miller T and Tan K H 1984 *Phys. Rev.* B **30** 2163
[28] Brydson R, Bruley J and Thomas J 1988 *Chem. Phys. Lett.* **149** 343
[29] Miyano K E, Ederer D L, Callcott T A, Dong Q Y, Jia J J, Zhou L and Mueller D R 1994 *Phys. Rev.* B **49** 5929
[30] Soininen J A, Hämäläinen K, Caliebe W A, Kao C-C and Shirley E L 2001 *J. Phys.: Condens. Matter* **13** 8039
[31] Tsuji J, Kojima K, Ikeda S, Nakamatsu H, Mukoyama T and Taniguchi K 2001 *J. Synchrotron Radiat.* **8** 554
[32] Tsuji J, Nakamatsu H, Mukoyama T, Kojima K, Ikeda S and Taniguchi K 2002 *X-Ray Spectrom.* **31** 319
[33] Handa K, Kojima K, Ozutsumi K, Taniguchi K and Ikeda S 2005 *Memoires Sr. Center Ritsumeikan Univ.* **7** 3
[34] Albrecht S, Onida G and Reining L 1997 *Phys. Rev.* B **55** 10278
[35] Jiang N and Spence J C H 2004 *Phys. Rev.* B **69** 115112
[36] Mauchamp V, Boucher F, Ouvrard G and Moreau P 2006 *Phys. Rev.* B **74** 115106
[37] Mauchamp V, Moreau P, Ouvrard G and Boucher F 2008 *Phys. Rev.* B **77** 045117
[38] Onida G, Reining L and Rubio A 2002 *Rev. Mod. Phys.* **74** 601
[39] Puschnig P 2002 Excitonic effects in organic semi-conductors *PhD Thesis* Karl-Franzens-Universität Graz (Aachen: Shaker)
[40] Albrecht S, Reining L, Del Sole R and Onida G 1998 *Phys. Rev. Lett.* **80** 4510

[41] Benedict L X, Shirley E L and Bohn R B 1998 *Phys. Rev. Lett.* **80** 4514
[42] Rohlfing M and Louie S G 1998 *Phys. Rev. Lett.* **81** 2312
[43] Rohlfing M and Louie S G 2000 *Phys. Rev.* B **62** 4927
[44] Arnaud B and Alouani M 2001 *Phys. Rev.* B **63** 085208
[45] Singh D J and Nordström L 2006 *Planewaves, Pseudopotentials and the LAPW Method* 2nd edn (Berlin: Springer)
[46] Madsen G K H, Blaha P, Schwarz K, Sjöstedt E and Nordström L 2001 *Phys. Rev.* B **64** 195134
[47] Perdew J P, Burke K and Ernzerhof M 1996 *Phys. Rev. Lett.* **77** 3865
[48] Fetter A L and Walecka H D 1971 *Quantum Theory of Many-Particle Systems* (New York: McGraw-Hill) (2003 (Mineola: Dover) reprint)
[49] Marini A and del Sole R 2003 *Phys. Rev. Lett.* **91** 176402